Spatial proteomics

Investigating the colon adenocarcinoma tumor microenvironment with spatial biology antibody conjugates and the EVOS S1000 Spatial Imaging System

Introduction

Colorectal cancer (CRC) is the second-leading cause of cancer deaths globally, with incidence rates that are increasing among younger adults, making it a high research priority. A key challenge in CRC research is tumor heterogeneity [1]. Colorectal tumors exhibit high interpatient variability and high intratumor heterogeneity, as distinct mutational states and microenvironments can be present in different locations in the same tumor. This complexity makes it difficult to develop precise therapies and predict patient treatment responses, so a better understanding of the unique molecular and structural characteristics of CRC tumors is needed.

Spatial biology is transforming pathology and cancer biology research by enabling high-plex molecular characterization in the physiological context of intact tissue microenvironments. This spatial dimension provides insight into how biological processes are influenced by their cellular environments, which is often missed in conventional single-cell analyses. For example, human tumors often contain infiltrates of immune cells, and researchers have identified correlations between patient outcomes and the density of specific immune cell populations in tumors and the invasive margins around them [2,3]. These immune cell subtypes express protein-specific biomarkers or combinations of biomarkers that can be detected via immunohistochemical (IHC) tissue labeling and imaging. High-plex IHC labeling and compatible fluorescence detection platforms are central to this approach, enabling detailed characterization of tissue microenvironments in human tumors.

Despite its potential, high-plex labeling with fluorescent dyes can be time-consuming and involve multiple rounds of staining, stripping, and imaging. Complex and nonintuitive imaging platforms can pose additional challenges in spatial proteomics experiments. The Invitrogen™ EVOS™ S1000 Spatial Imaging System addresses these challenges with a streamlined image acquisition workflow and user-friendly interface. This easy-to-use spatial imaging platform is capable of simultaneous imaging of up to nine biomolecules when used with trusted Invitrogen™ Alexa Fluor™ and Alexa Fluor™ Plus primary antibody conjugates or Invitrogen™ Aluora™ reagents, offering a comprehensive solution for spatial proteomics imaging.

Here we outline the spatial proteomics imaging workflow for the EVOS S1000 Spatial Imaging System, including sample preparation, image acquisition, and subsequent analysis of immune cell populations in normal colon and colon adenocarcinoma tissues.

Materials and methods

Multiplex panel and single-color control preparation

Normal human colon and colon adenocarcinoma tissues were sourced from different donors and used to generate 9-plex data on the EVOS S1000 Spatial Imaging System. From each tissue source, the following types of samples were prepared:

- A 9-plex sample stained with eight primary antibody conjugates (Table 1) and DAPI nuclear counterstain
- A single-color control (SCC) sample for each of the nine probes to build the spectral unmixing matrix
- An unstained tissue sample to correct for background fluorescence

IHC and staining conditions

The formalin-fixed, paraffin-embedded (FFPE) tissue sections were subjected to a standard xylene deparaffinization and rehydration protocol, followed by heat-induced epitope retrieval in a pressure cooker with citraconic anhydride antigen retrieval solution for 20 minutes. White-light photobleaching to reduce tissue autofluorescence was performed using a modified version of a previously described protocol [4]. The tissue samples were placed in a transparent reservoir containing a solution of 24 mM NaOH and 4.5% H_2O_2 in PBS, and illuminated with white light for 30 minutes. The samples were then permeabilized with 0.1% Triton™ X-100 in PBS for 30 minutes and blocked with 3% BSA and 5% NGS for 1 hour at room temperature.

The primary antibodies were diluted in 3% BSA and added to the samples in a humidified chamber, and the samples were incubated overnight at 4°C. DAPI nuclear counterstain was applied to the multiplex samples and the DAPI-only SCCs. The samples were then covered with coverslips, mounted with Invitrogen™ ProLong™ Glass Antifade Mountant, and cured overnight at room temperature. Whole-tissue area scans were imaged, stitched, and spectrally unmixed on the EVOS S1000 Spatial Imaging System using the 20x objective with 0.325 µm/pixel resolution.

Image analysis

The Highplex FL module (version 4.2.14) in HALO™ software (version 4.0.5107.318) was used for cellular phenotyping. For cell segmentation, the DAPI channel was used to detect cell nuclei with the minimum nuclear intensity threshold value set to 0.01 and the maximum value set to 1 to capture all nuclei. The aggressiveness of nuclear segmentation was set high (0.9) to break up cell clumps. To define cell size, an expansion radius from the nucleus was set to a low value (1), since the cells were not much larger than nuclei. Cell identities for membrane markers CD68, CD20, CD4, and CD8 were scored according to a positive threshold set on the cytoplasmic signal and nuclear signal for nuclear markers Ki-67 and FOXP3. Double-positive status for Ki-67 and an additional marker was the criterion for scoring proliferating cells.

Results

High-plex EVOS S1000 workflow

Panels of up to eight directly conjugated primary antibodies and DAPI can be multiplexed in a single incubation step, followed by detection via spectral unmixing to enable single-cell detection of markers across whole tissues (Figure 1). The linear spectral unmixing algorithm takes reference spectra of tissue autofluorescence and each fluorophore from SCCs to create a custom unmixing matrix, then seamlessly resolves each marker from the crowded spectral environment post-acquisition (Figure 2). In this study, we performed 9-plex staining and analysis with human healthy colon and colon adenocarcinoma tissues.

Table 1. Invitrogen™ antibody–dye conjugates in the 9-plex panel.

Primary antibody conjugate	Target intensity	Fluorophore strength	Cell type	Dilution	Working concentration
Alpha-Smooth Muscle Actin Monoclonal Antibody (1A4), Alexa Fluor™ 420	+++	+	Smooth muscle cell	1:50	4 µg/mL
CD68 Monoclonal Antibody (KP1), Alexa Fluor™ Plus 488	+++	+++	Macrophage	1:20	10 µg/mL
CD20 Monoclonal Antibody (L26), Alexa Fluor™ 514	+++	++	B cell	1:20	10 µg/mL
CD4 Monoclonal Antibody (N1UG0), Alexa Fluor™ Plus 555	++	++	Helper T cell	1:10	20 µg/mL
CD8 Alpha Monoclonal Antibody (C8/144B), Alexa Fluor™ Plus 594	+	+++	Cytotoxic T cell	1:20	10 µg/mL
FOXP3 Monoclonal Antibody (PCH101), Alexa Fluor™ Plus 647	+	+++	Regulatory T cell	1:10	20 µg/mL
Pan-Cytokeratin Monoclonal Antibody (AE1/AE3), Alexa Fluor™ 700	+++	+	Epithelial cell	1:50	4 µg/mL
Ki-67 Monoclonal Antibody (SolA15), Alexa Fluor™ Plus 750	+++	+	Proliferating cell	1:10	20 µg/mL

Spatial multiplex spectral imaging workflow

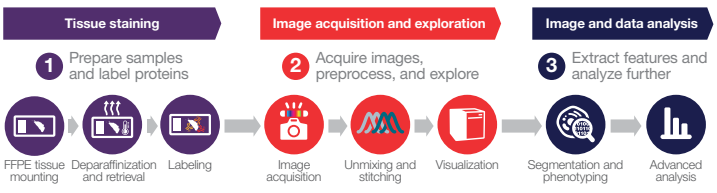

Figure 1. Overview of the EVOS S1000 workflow using primary antibody conjugates. Design a panel with primary antibody conjugates, then (1) stain tissue with up to eight markers plus DAPI and (2) image and spectrally unmix whole-tissue slices.

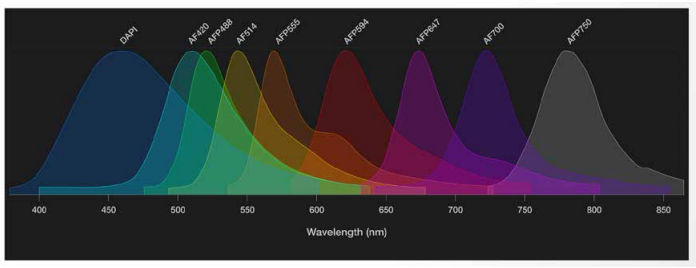

Figure 2. Fluorophore emission spectra of primary antibody conjugates in a 9-plex panel. The relative fluorescence intensity for each fluorophore in the 9-plex panel is plotted by wavelength. The spectra display extensive overlap, which requires spectral unmixing to resolve.

Imaging of 9-plex colon panels on the EVOS S1000 Spatial Imaging System

We imaged whole-tissue scans of the 9-plex panel on the normal colon and colon adenocarcinoma samples using the EVOS S1000 Spatial Imaging System, which revealed significant structural differences between the tissues. In the normal colon scan (Figure 3A), we identified the three main structural layers (green arrows): the inner mucosa layer containing crypts responsible for water and nutrient uptake; the muscularis externa layer, seen as a large band of smooth muscle enveloping the mucosa to move digested food along the intestinal tract; and the submucosa layer between the two layers, composed of connective tissue and blood vessels visible as round structures labeled with α-SMA. We also identified two immune cell clusters containing $CD20^+$ B cells and $CD4^+/CD8^+$ T cells (white arrows). The close-up view of the colon crypts, in Figure 3B, shows interspersed macrophages, other immune cells, and proliferating stem cell niches marked by Ki-67 that continuously replenish the intestinal epithelium.

In contrast, the colon cancer sample displayed a well-differentiated adenocarcinoma with tumor tissue composed of irregular, uncontrollably growing glandular crypt-like structures infiltrating multiple layers of the bowel wall (Figure 3C). The macro-scale tumor features included blood vessels scattered throughout the tissue, visualized as circular α-SMA staining structures (white arrows). A tertiary lymphoid structure (TLS) was also identified in the top left corner of the tumor section (yellow oval). Tertiary lymphoid structures are dense clusters of immune cells that can form near chronically inflamed or tumorous tissues [5]. By focusing in on a section of the tissue, we could detect infiltrating and irregular glandular structures marked by pan-cytokeratin (pan-CK) as well as a large number of $CD68^+$ tumor-associated macrophages (Figure 3D). These datasets demonstrate the power of high-plex IHC labeling with primary antibody conjugates and high-resolution full-tissue imaging for characterizing tissue structures and tumor microenvironments.

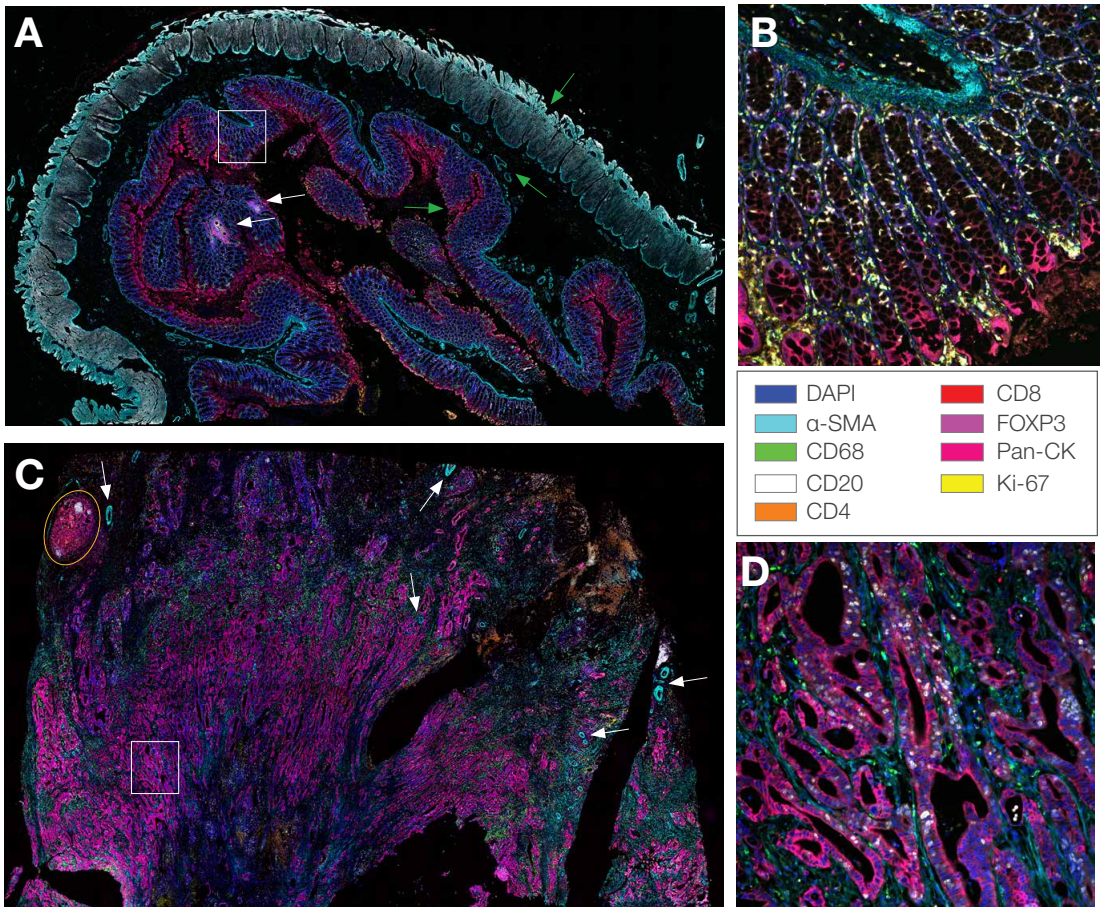

Figure 3. Images of normal colon and adenocarcinoma tissues stained with the 9-plex colon panel. (A) Unmixed whole-tissue scan of normal colon tissue collected using the 20x objective on the EVOS S1000 system. The green arrows point to the three main structural layers of the colon. The top arrow marks the muscularis externa; the middle arrow marks the submucosa; and the bottom arrow marks the mucosa. The white arrows point to immune cell clusters, and the white box marks the location of the single field of view (FOV) shown in B. **(B)** Single 20x FOV image of healthy crypt structures in normal colon tissue. **(C)** Unmixed whole-tissue scan of colon adenocarcinoma tissue. The yellow oval denotes the location of a tertiary lymphoid structure (TLS), and the white arrows denote blood vessels labeled with α-SMA monoclonal antibody Alexa Fluor 420 conjugate. The white box marks the location of the single FOV shown in D. **(D)** Single 20x FOV image of abnormal tumor glandular structures in the adenocarcinoma tissue.

Cellular phenotyping of normal colon and colon adenocarcinoma tissues

Cellular phenotyping involves the identification and quantitation of cell types at the single-cell level within the spatial context of tissue samples, which is crucial for understanding disease mechanisms and treatment responses. We used HALO software to analyze the colon imaging data, which involved three main steps: nuclear detection and cell segmentation; classification of cells as being positive or negative for each marker; and definition and identification of cellular phenotypes. Cell nuclei were identified and segmented using the DAPI channel, followed by cell boundary expansion using the HALO AI Nuclei Seg V2 algorithm. Threshold adjustment for each marker helped us accurately score cells, and phenotypes were defined based on marker presence to identify specific cell subpopulations (Figure 4).

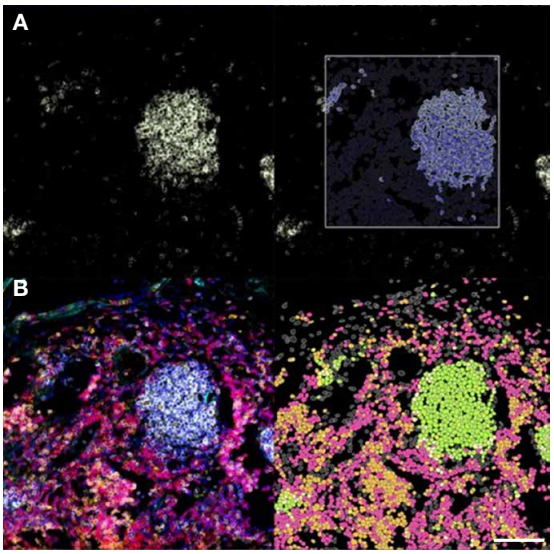

Figure 4. Nuclear segmentation, marker thresholding, and cellular phenotyping in HALO software. (A) Left panel: fluorescence from cells labeled with Alexa Fluor 514 CD20 monoclonal antibody conjugate. Right panel: positive signal threshold applied to CD20 in a window within the FOV. **(B)** Left panel: multiplex fluorescence FOV. Right panel: cell phenotypes found within the multiplex, coded by color. Scale bar: 100 µm.

We analyzed the proportion of each immune cell subtype identified using the antibody conjugate panel relative to the total cells detected, and we found that immune cells constituted a relatively small portion (~10%) of the total cells in both samples (Figure 5A). This is to be expected, as enterocytes, smooth muscle cells, goblet cells, and others constitute the majority of cells in the colon. The greatest difference in immune cell content was a nearly 10-fold increase in the percentage of macrophages in the tumor relative to in the normal tissue. Tumor-associated macrophages are known to promote tumor growth by angiogenesis, and they are key contributors to cancer-related inflammation [6]. We also examined the percentage of each cell type undergoing proliferation and observed a greater than 100-fold increase in regulatory FOXP3$^+$ and CD4$^+$ T (Treg) cell proliferation in the tumor relative to in the normal tissue (Figure 5B). An increase in Treg cells in colorectal tumors can promote tumor development and immunotherapy failure, which is associated with a poorer prognosis [7].

The tertiary lymphoid structure (TLS) in Figure 5C was identified in the full tissue scan of the adenocarcinoma sample. TLSs are thought to play an important role in the immune response to colorectal cancers and are linked to better prognostic outcomes [8,9]. We performed a cellular composition analysis using a modified version of a previously described protocol [10] to characterize the tumor TLS, and found that 62% of the cells were cytotoxic T cells, 24.5% were helper T cells, and 13.5% were B cells. The most abundant cell type, CD8$^+$ cytotoxic T cells, is a key contributor to the anti-tumor immune response. Macrophages and Treg cells both made up less than 1% of the TLS (Figure 5D). Together, these data offer insights into the capabilities of cellular phenotyping and spatial analysis using multiplex imaging data collected with the EVOS S1000 Spatial Imaging System.

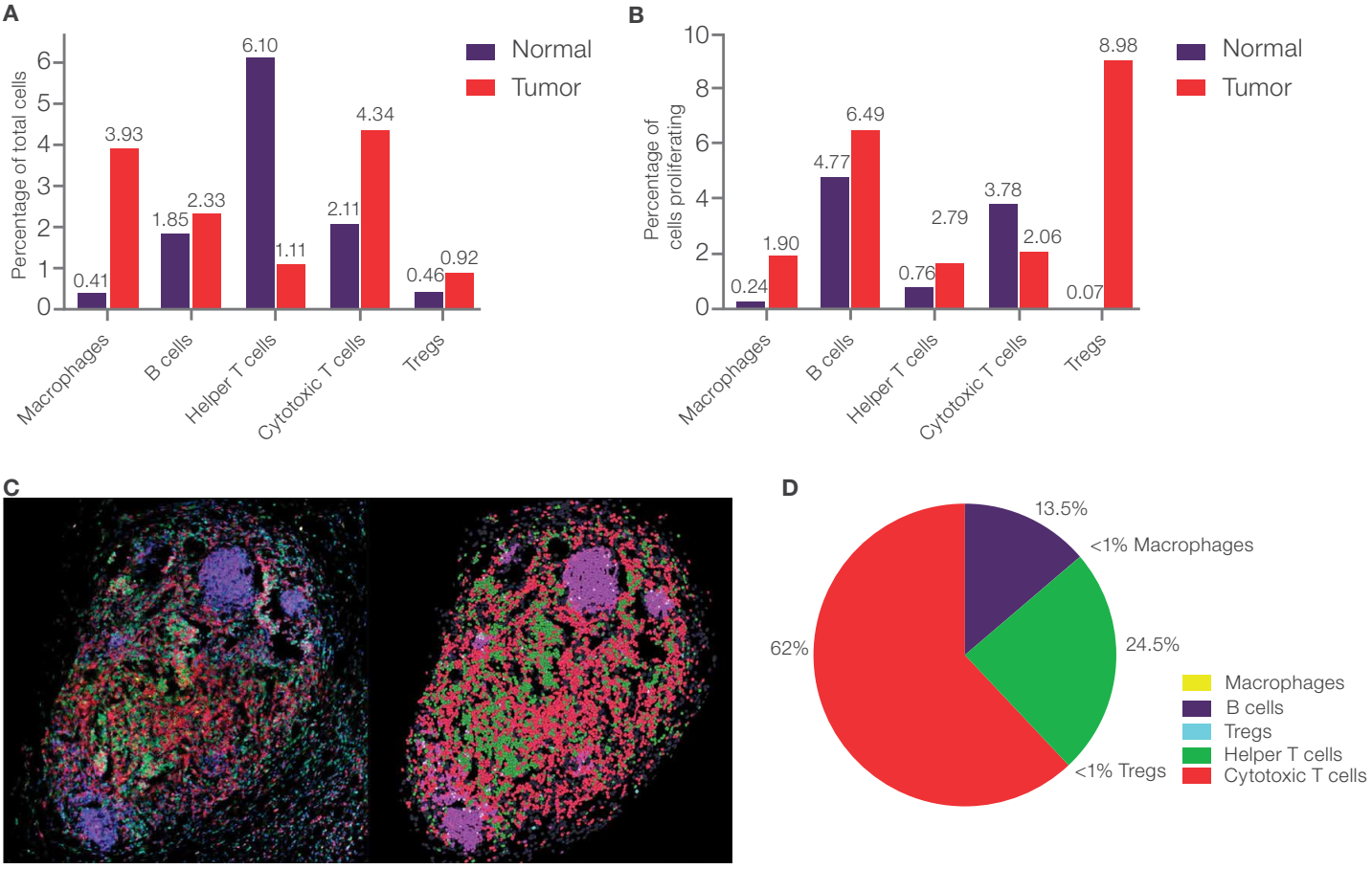

Figure 5. Cellular phenotyping of whole tissues and an adenocarcinoma tumor tertiary lymphoid structure. (A) Percentage of each cell type observed in whole-tissue scans of healthy and tumor colon tissue. **(B)** Percentage of each cell type observed proliferating in healthy and tumor colon whole-tissue scans. **(C)** Left panel: close-up of the colon adenocarcinoma tertiary lymphoid structure (TLS) outlined by the yellow oval in Figure 3C. The markers are pseudo-colored to be consistent with those shown in D. Right panel: cells identified within the TLS after nuclear segmentation and cellular phenotyping in HALO software. **(D)** Cellular composition of the colon adenocarcinoma TLS.

Conclusion

Incorporating advanced staining, imaging, and analysis techniques into a multiplex workflow with the EVOS S1000 Spatial Imaging System provided detailed insights into tissue structure and cellular phenotypes. The data collected in this study highlight significant differences between normal colon and colon adenocarcinoma tissues and underscore the utility of the EVOS S1000 Spatial Imaging System and primary antibody conjugates for characterizing tumor microenvironments and immune responses.

References

1. González NS, Salvà F, Ros J et al. (2023) Unravelling the complexity of colorectal cancer: heterogeneity, clonal evolution, and clinical implications. *Cancers* 15(16):4020. doi: 10.3390/cancers15164020
2. Galon J, Costes A, Sanchez-Cabo F et al. (2006) Type, density, and location of immune cells within human colorectal tumors predict clinical outcome. *Science* 313(5795):1960–1964. doi: 10.1126/science.1129139
3. Fridman WH, Pagès F, Sautès-Fridman C, Galon J (2012) The immune contexture in human tumours: impact on clinical outcome. *Nat Rev Cancer* 12:298–306. doi: 10.1038/nrc3245
4. Lin J-R, Izar B, Wang S et al. (2018) Highly multiplexed immunofluorescence imaging of human tissues and tumors using t-CyCIF and conventional optical microscopes. *eLife* 7:e31657. doi: 10.7554/eLife.31657
5. Wang Q, Zhong W, Shen X et al. (2024) Tertiary lymphoid structures predict survival and response to neoadjuvant therapy in locally advanced rectal cancer. *npj Precis Onc* 8:61. doi: 10.1038/s41698-024-00533-w
6. Chen Y, Song Y, Du W et al. (2019) Tumor-associated macrophages: an accomplice in solid tumor progression. *J Biomed Sci* 26:78. doi: 10.1186/s12929-019-0568-z
7. Aristin Revilla S, Kranenburg O, Coffer PJ (2022) Colorectal cancer-infiltrating regulatory T cells: functional heterogeneity, metabolic adaptation, and therapeutic targeting. *Front Immunol* 13:903564. doi: 10.3389/fimmu.2022.903564
8. Wang Q, Shen X, An R et al. (2022) Peritumoral tertiary lymphoid structure and tumor stroma percentage predict the prognosis of patients with non-metastatic colorectal cancer. *Front Immunol* 13:962056. doi: 10.3389/fimmu.2022.962056
9. Sautès-Fridman C, Petitprez F, Calderaro J et al. (2019) Tertiary lymphoid structures in the era of cancer immunotherapy. *Nat Rev Cancer* 19:307–325. doi: 10.1038/s41568-019-0144-6
10. Schürch CM, Bhate SS, Barlow GL et al. (2020) Coordinated cellular neighborhoods orchestrate antitumoral immunity at the colorectal cancer invasive front. *Cell* 182(5):1341–1359. doi: 10.1016/j.cell.2020.10.021

Ordering information

Description	Cat. No.
Imaging system	
EVOS S1000 Spatial Imaging System	AMFS1000
Spatial biology–verified antibody conjugates	
Alpha-Smooth Muscle Actin Monoclonal Antibody (1A4), Alexa Fluor 420	758-9760-82
CD68 Monoclonal Antibody (KP1), Alexa Fluor Plus 488	752-0688-82
CD20 Monoclonal Antibody (L26), Alexa Fluor 514	753-0202-94
CD4 Monoclonal Antibody (N1UG0), Alexa Fluor Plus 555	754-2444-82
CD8 alpha Monoclonal Antibody (C8/144B), Alexa Fluor Plus 594	755-0085-82
FOXP3 Monoclonal Antibody (PCH101), Alexa Fluor Plus 647	756-4776-82
Pan-Cytokeratin Monoclonal Antibody (AE1/AE3), Alexa Fluor 700	56-9003-82
Ki-67 Monoclonal Antibody (SolA15), Alexa Fluor Plus 750	757-5698-82
Reagents	
DAPI solution, 1 mg/mL	62248
ProLong Glass Antifade Mountant	P36980
PBS, pH 7.4	10010049

Learn more at **thermofisher.com/evoss1000**

invitrogen